

Supplementary Information for

**Computationally designed pyocyanin demethylase acts synergistically with tobramycin to kill recalcitrant *Pseudomonas aeruginosa* biofilms**

Chelsey M. VanDriss<sup>a</sup>, Rosalie Lipsh-Sokolik<sup>b</sup>, Olga Khersonsky<sup>b</sup>, Sarel J. Fleishman<sup>b\*</sup>, Dianne K. Newman<sup>a,c\*</sup>

<sup>a</sup>*Division of Biology and Biological Engineering and* <sup>c</sup>*Division of Geological and Planetary Sciences, California Institute of Technology, Pasadena, CA, USA*

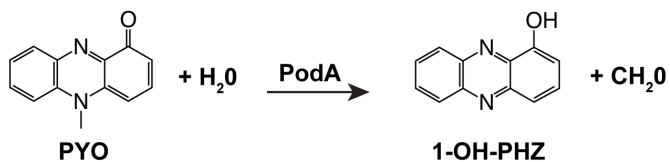
<sup>b</sup>*Department of Biomolecular Sciences, Weizmann Institute of Science, Rehovot, Israel*

Correspondence: Sarel J. Fleishman or Dianne K. Newman  
Emails: sarel.fleishman@weizmann.ac.il, dkn@caltech.edu

**This PDF file includes:**

Figures S1 to S11  
Tables S1 to S3  
SI References

A



B

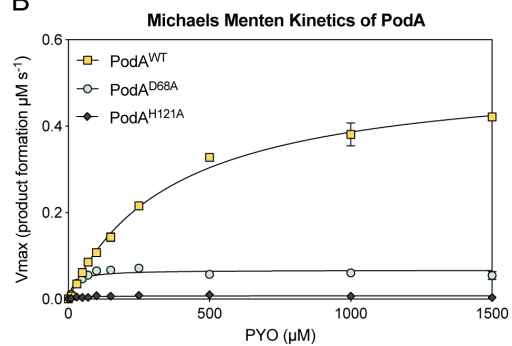


**Figure S1. PodA reaction and kinetics.** (A) PodA reaction schematic of PYO conversion to 1-OH-PHZ. PYO, pyocyanin; 1-OH-PHZ, 1-hydroxyphenazine. (B) PodA ( $3 \mu\text{M}$ ) and PYO (concentrations indicated on  $x$ -axis) were incubated and monitored at  $690 \text{ nm}$ .  $V_{max}$  values were plotted against  $[\text{PYO}]$  and  $K_M$  was calculated by fitting data to the Michaelis-Menten equation as indicated by black line. Each data point represents the mean of three replicates and error bars represent standard deviation.

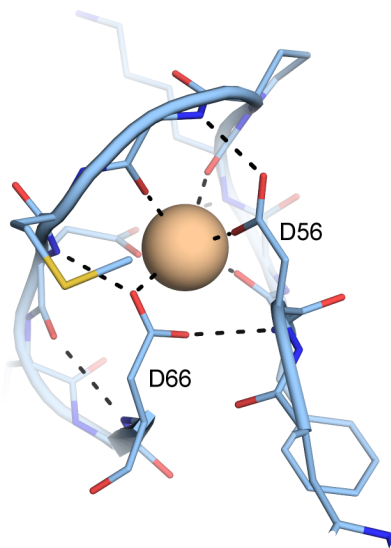


**Figure S2.  $\text{Ca}^{2+}$  ion binding site of PodA.** The loop between residues 56-66 connecting the ends of anti-parallel  $\beta$ -strands is stabilized through multiple bonds between a  $\text{Ca}^{2+}$  ion and loop backbone atoms and sidechains, mainly through Asp56 and Asp66. This  $\text{Ca}^{2+}$  ion was present in the crystal structure upon which our design calculations were based, likely due to the crystal having formed in a buffer that contained calcium (3).

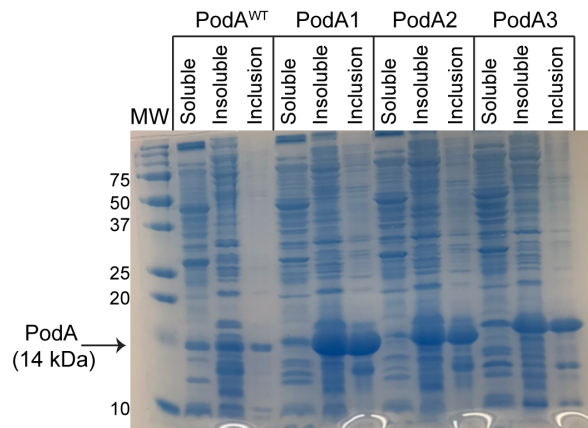


**Figure S3. Gel electrophoresis of PodA<sup>WT</sup> and protein design variants of PodA overexpression cultures.** Inclusion bodies from overexpression cultures of designed variants were analyzed using BugBuster<sup>TM</sup>. A representative SDS-PAGE gel is shown for PodA1-PodA3. Precision Plus Protein<sup>TM</sup> used as a MW marker (lane 1), with relevant molecular weights designated.

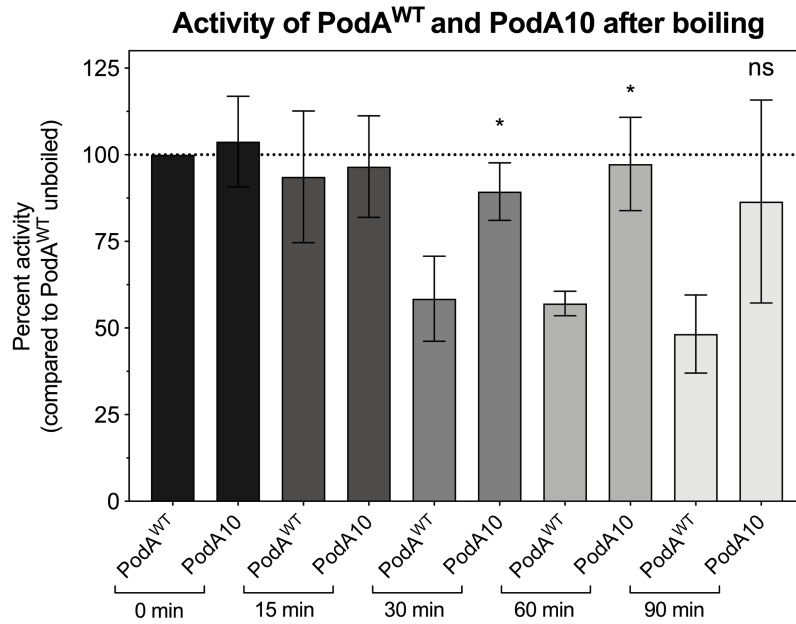


**Figure S4. Activity of WT PodA<sub>30-162</sub> and PodA10 after boiling.** Protein was boiled as described in Materials and Methods, followed by an activity assay with PodA (3  $\mu$ M) and PYO (100  $\mu$ M) in a Spectramax M3 plate reader monitoring PYO absorbance (690 nm) overtime. Specific activity ( $\text{nmol min}^{-1} \text{mg}^{-1}$ ) was calculated for each sample. Replicates of PodA<sup>WT</sup> un-boiled were averaged and set to 100% activity (dashed line). All other activities of boiled samples were compared to this value and presented as a percentage. Data represent technical triplicates and error bars represent standard deviation. A t-test was completed, with \* representing a  $p$ -value  $< 0.05$  and ns representing not significant.

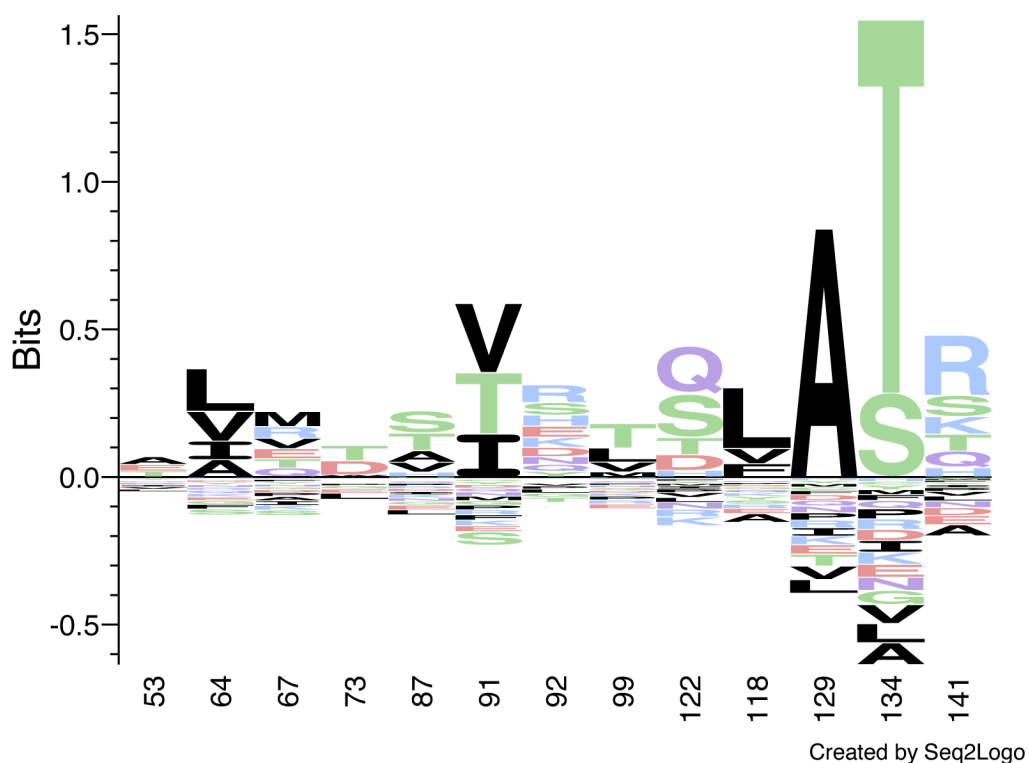


**Figure S5. Sequence logo of diversified positions.** Sequence logo representing residue observations in evolutionary analysis, generated with default parameters using <http://www.cbs.dtu.dk/biotools/Seq2Logo/> (1). Most successful designs did not use the most conserved residue in each position. For example, both PodA8 and PodA10 incorporated A53N, although Ala, Glu and Thr are evolutionarily more likely for this position. In addition, in position 129 the only preferable amino acid is Ala, but PodA8 and PodA10 mutated to A129V and A129T, respectively.

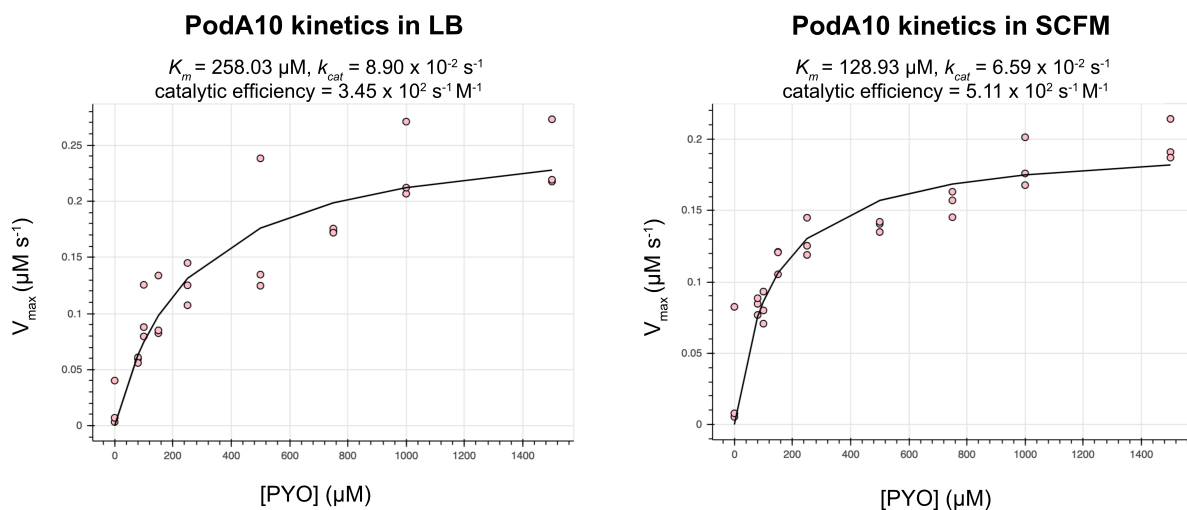
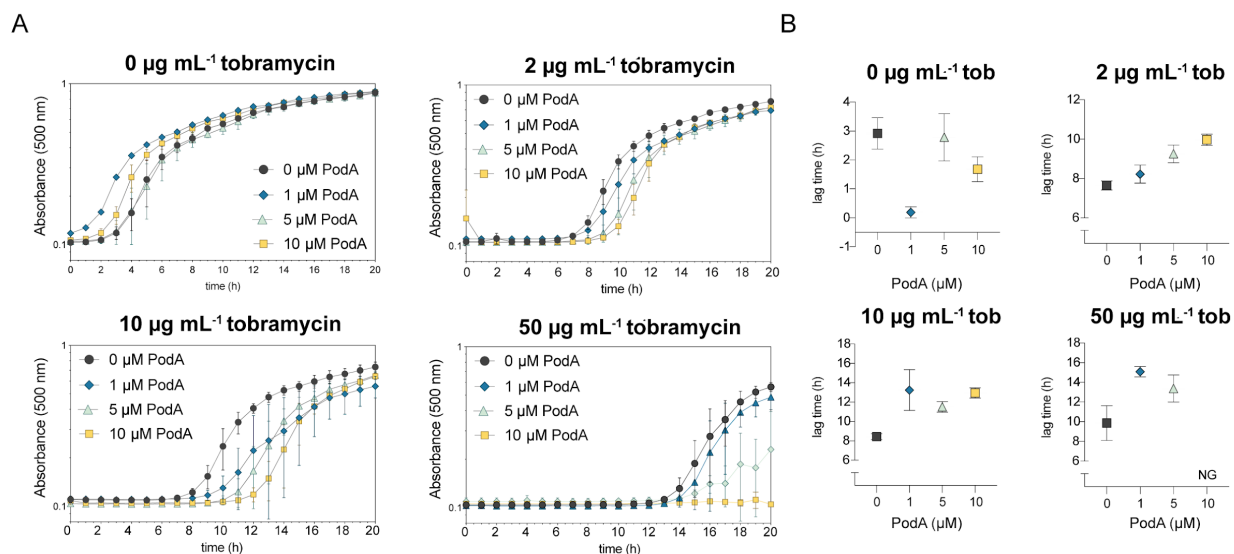


**Figure S6. Kinetics of PodA in growth media.** Using a continuous spectrophotometric assay as described in the Material and Methods, PodA (3  $\mu\text{M}$ ) and PYO (concentrations indicated on  $x$ -axis) were incubated and monitored at 690 nm.  $V_{max}$  values were plotted against [PYO] and an  $K_M$  was calculated by fitting data to the Michaelis-Menten equation as indicated by black line. Each data point represents the mean of three replicates. LB; lysogeny broth, SCFM; synthetic cystic fibrosis medium.

## Lysogeny Broth (LB)



## Synthetic Cystic Fibrosis Medium (SCFM)

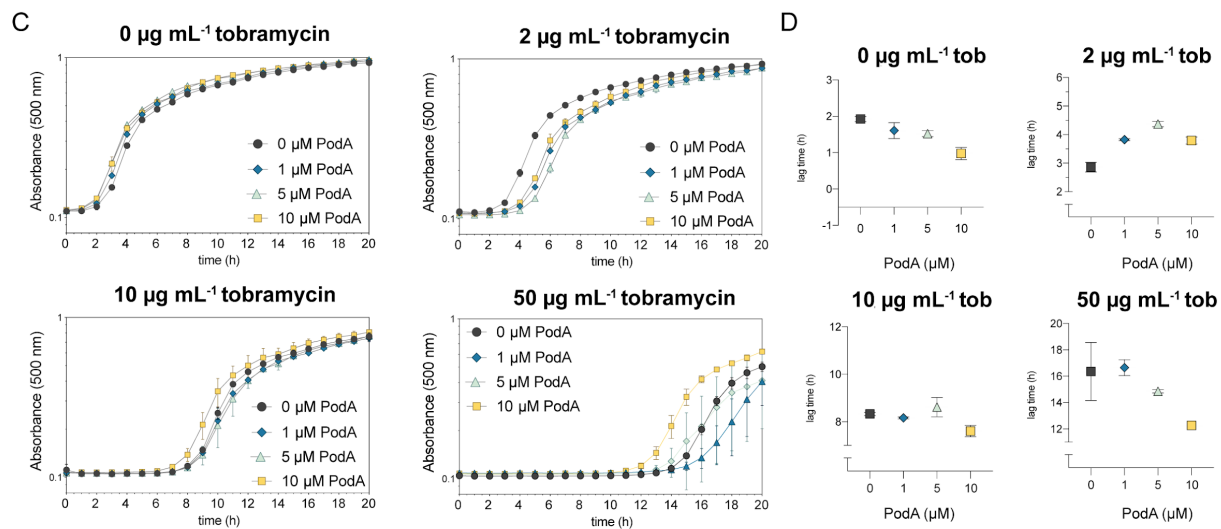


**Figure S7. *Pseudomonas PodA10* and antibiotic synergy experiments in LB and SCFM.** Growth curves represent outgrowth of cells that were incubated in LB (A) or SCFM (C) with PodA and no tobramycin (top left), or varying amounts of tobramycin (indicated in titles). Buffer was added in lieu of protein for 0  $\mu\text{M}$  PodA controls. Growth was monitored at OD<sub>500</sub> over time using a BioTek Plate Reader. Experiment was repeated in triplicate with a representative graph shown. Error bars represent the standard error of the mean of triplicates. B) and D) Lag times of cultures were calculated from growth curves in respective panels. Data were fit to the Gompertz curve-fitting model using Growth Curve Fitting program in R ([https://scott-h-saunders.shinyapps.io/gompertz\\_fitting\\_0v2/](https://scott-h-saunders.shinyapps.io/gompertz_fitting_0v2/)). Data represent the mean and standard error of triplicates. NG; no growth.



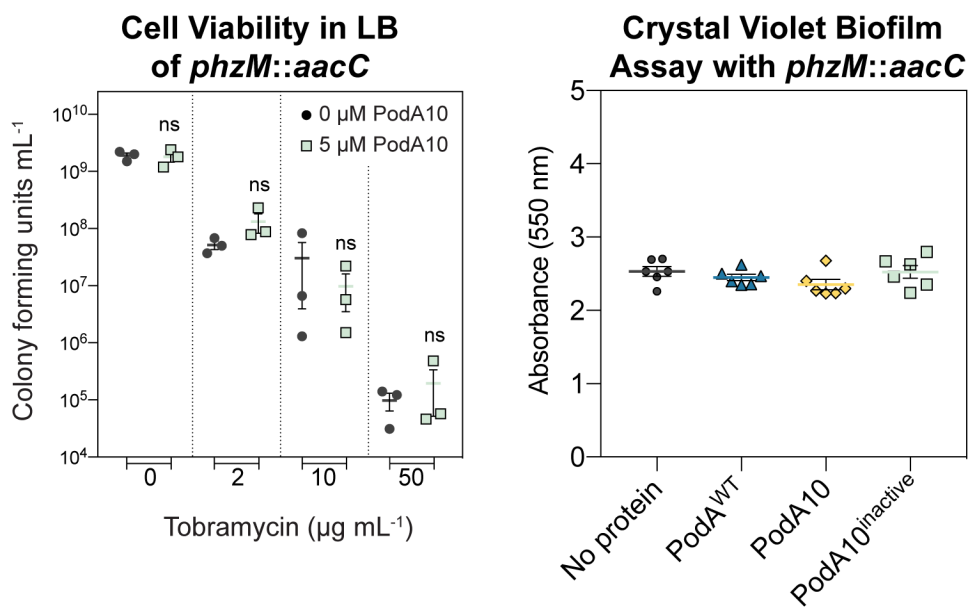


**Figure S8. Cell viability counts of *P. aeruginosa* cells that are unable to synthesize PYO.** A) The *P. aeruginosa* strain lacking *phzM* (a gene encoding the enzyme PhzM, a S-adenosylmethionine-dependent N-methyltransferase, that converts phenazine-1-carboxylic acid to the PYO precursor, 1-Me-PCA) was grown to stationary phase and incubated with PodA10 (0 μM or 5 μM) and tobramycin (concentrations indicated on x-axis) for LB. Data represent the mean of biological triplicates with error bars representing the standard error of the mean. B) *P. aeruginosa* cells were inoculated in a 96-well polystyrene plate containing minimal medium with arginine (40 mM) and either no PodA, WT PodA<sub>30-162</sub>, PodA10, or inactive PodA10 (i.e. PodA10<sup>H121A,E154A,Y156A</sup>), followed by incubation at 37 °C. After 24 h of growth, planktonic cells were washed away, and attached cells were stained with crystal violet, de-stained, and absorbance was measured at 550 nm. Error bars represent standard error of the mean. *aacC*, gentamicin N-acetyltransferase.

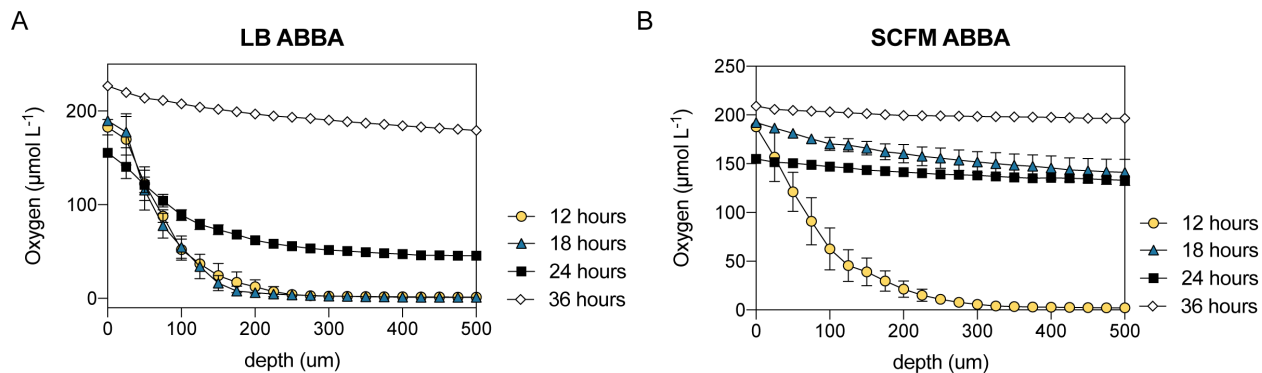


**Figure S9. *Pseudomonas* LB and SCFM ABBA oxygen profiles.** Cells were inoculated in LB or SCFM ABBA and grown for the time indicated in graph legends. Oxygen profiles were determined using a micrometer oxygen sensor (UniSense). All time points consisted of biological triplicates with technical triplicate readings of each ABBA block with error bars representing standard deviation. A) Oxygen profile time course of LB ABBA. B) Oxygen profile time course of SCFM ABBA.

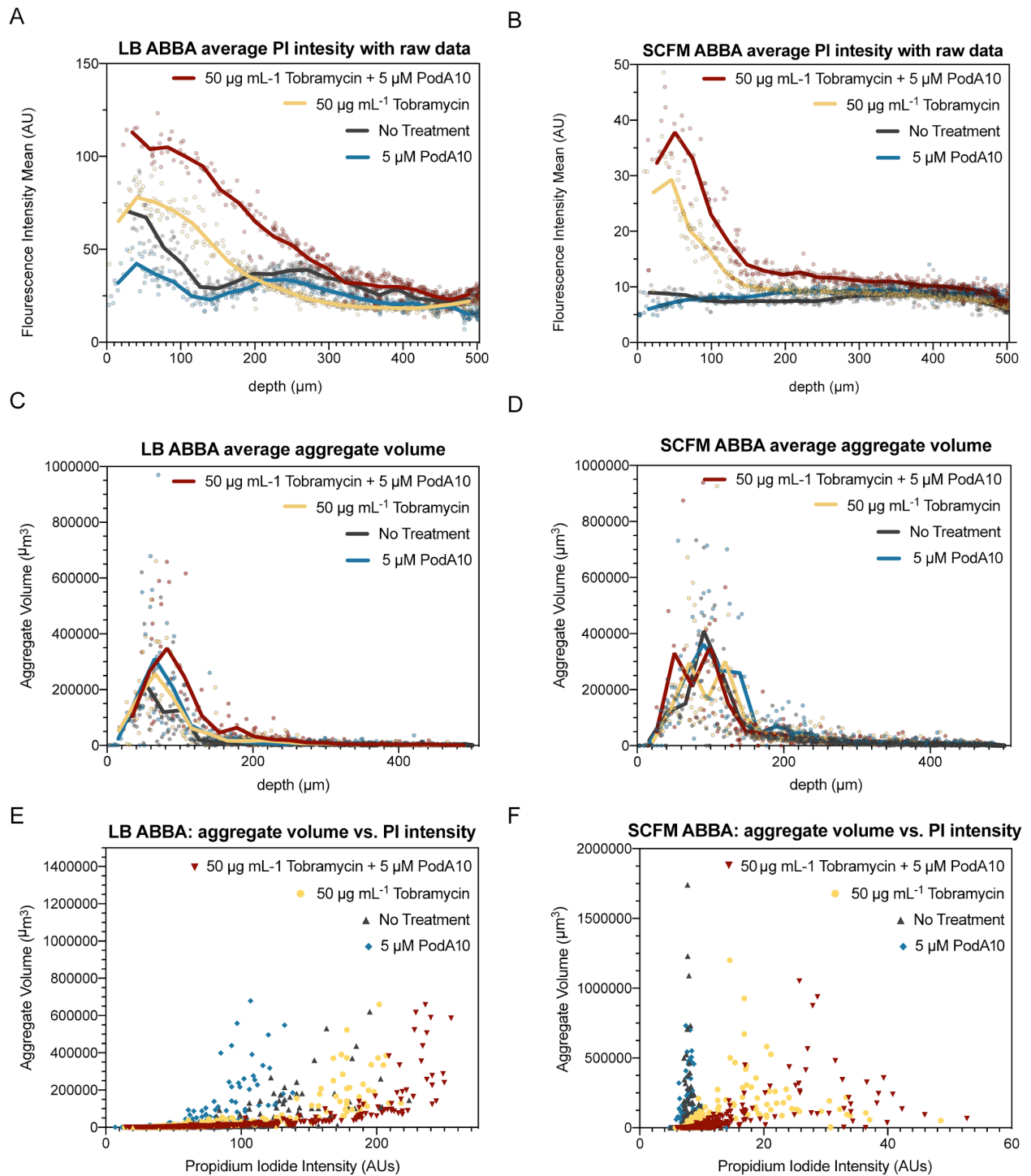


**Figure S10. *Pseudomonas* LB and SCFM ABBA aggregate volume analyses.** ABBA data from Fig. 4 were analyzed in Imaris to obtain PI mean intensity for LB (A) and SCFM (B), along with the volume of each aggregate for LB (C) and SCFM (D). Each point represents a single aggregate. Mean aggregate volume was calculated with a bin size of 20 (every 25  $\mu\text{m}$ ) and plotted as a solid line. Propidium Iodide intensity from Fig. 4 was plotted against each aggregate volume for LB (E) and SCFM (F).

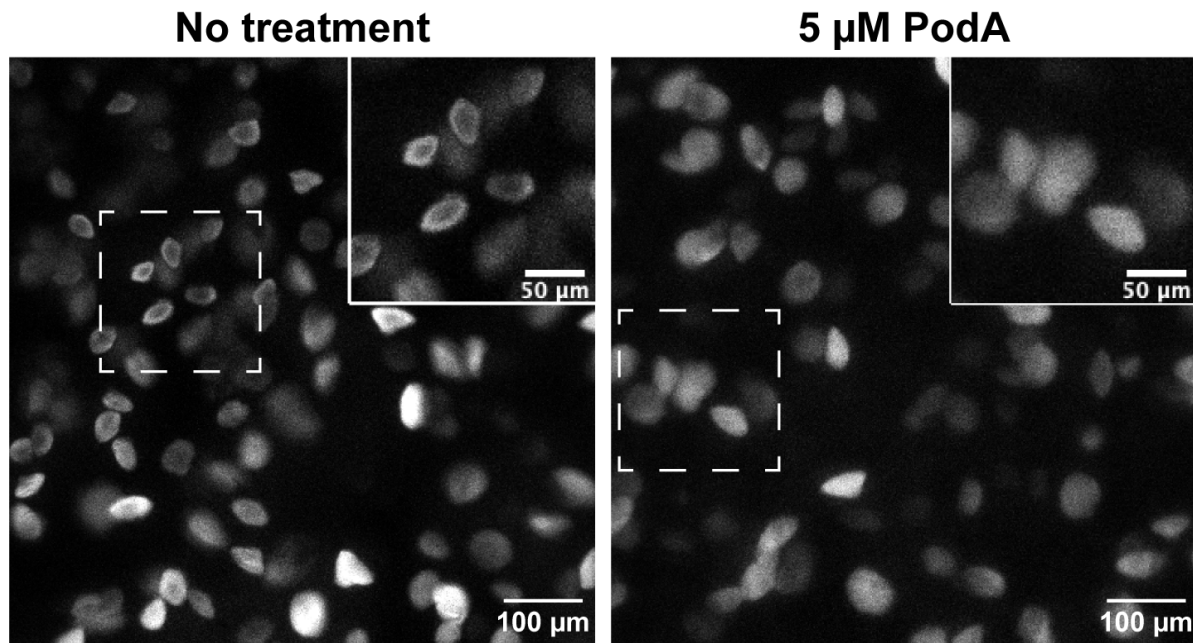


**Figure S11. Differences of PI staining in LB between untreated and PodA treated ABBAs.** Microscopy data LB ABBAs were analyzed in the XY-plane at 90 μm depth (stack 15/84), with brightness contrast normalized to the no treatment control. Example of ring staining pattern indicated by zooming in on dashed boxes, with zoomed in images in the upper right corner. Look up table (LUT) settings were normalized to no treatment condition.

<b>Table S1. Bacterial strains used in this study</b>		
<b>Strain</b>	<b>Relative Genotype</b>	<b>Source</b>
<b><i>E. coli</i> strains</b>		
<i>E. coli</i> DH5 $\alpha$	$\Phi$ 80dlacZ $\Delta$ M15 <i>recA1 endA1 gyrA96 thi-1 hsdR17</i> ( <i>r<sub>k</sub><sup>-</sup>, m<sub>k</sub><sup>+</sup></i> ) <i>supE44 relA1 deoR</i> $\Delta$ ( <i>lacZYA-argF</i> ) U169 <i>phoA</i>	NEB
<i>E. coli</i> BL21 ( $\lambda$ DE3)	B F <sup>-</sup> <i>ompT gal dcm lon hsdS</i> ( <i>r<sub>BMB</sub></i> ) <i>gal</i> ( $\lambda$ DE3)	NEB
<b><i>P. aeruginosa</i> strains</b>		
DKN263	<i>Pseudomonas aeruginosa</i> wildtype UCBPP-14	Lab Collection
DKN295	<i>Pseudomonas aeruginosa</i> <i>phzM::aacC</i>	Lab Collection

<b>Table S2. Plasmids used in this study</b>		
<b>Plasmid</b>	<b>Genotype</b>	<b>Source</b>
pTEV16	<i>lacI<sup>+</sup> bla<sup>+</sup></i>	(2)
<b>Overexpression plasmids</b>		
pET20b(+)- <i>podA</i> D68A	<i>M. fortuitum</i> PodA <sup>D68A</sup> in pET20b (+)	(3)
pET20b(+)- <i>podA</i> D72A	<i>M. fortuitum</i> PodA <sup>D72A</sup> in pET20b (+)	(3)
pET20b(+)- <i>podA</i> H121A	<i>M. fortuitum</i> PodA <sup>H121A</sup> in pET20b (+)	(3)
pET20b(+)- <i>podA</i> E154A	<i>M. fortuitum</i> PodA <sup>E154A</sup> in pET20b (+)	(3)
pET20b(+)- <i>podA</i> Y156A	<i>M. fortuitum</i> PodA <sup>Y156A</sup> in pET20b (+)	(3)
pPodA1	<i>Mycobacterium fortuitum podA</i> <sub>30-162</sub> <sup>+</sup> cloned into pTEV16 with a TEV cleavable 6X-His tag	This study
pPodA2	<i>Mycobacterium fortuitum podA</i> designed variant cloned into pTEV16 with a TEV cleavable 6X-His tag: I73K, A87V, T91V, M99T, A128V	This study
pPodA3	<i>Mycobacterium fortuitum podA</i> designed variant cloned into pTEV16 with a TEV cleavable 6X-His tag: I73T, A87V, T91V, M99V, A128V	This study
pPodA4	<i>Mycobacterium fortuitum podA</i> designed variant cloned into pTEV16 with a TEV cleavable 6X-His tag: I73K, A87V, M99T, A129V, K141T	This study
pPodA5	<i>Mycobacterium fortuitum podA</i> designed variant cloned into pTEV16 with a TEV cleavable 6X-His tag: I73E, A87V, M99I, A129V, K141T	This study
pPodA6	<i>Mycobacterium fortuitum podA</i> designed variant cloned into pTEV16 with a TEV cleavable 6X-His tag: I73L, A87I, M99V, A129V, K141T	This study
pPodA7	<i>Mycobacterium fortuitum podA</i> designed variant cloned into pTEV16 with a TEV cleavable 6X-His tag: I73R, A87V, T91V, M99V, A129T	This study
pPodA8	<i>Mycobacterium fortuitum podA</i> Sarel designed variant cloned into pTEV16 with a TEV cleavable 6X-His tag: I73L, A87I, T91V, M99T, A129V	This study
pPodA9	<i>Mycobacterium fortuitum podA</i> designed variant cloned into pTEV16 with a TEV cleavable 6X-His tag: A53N, I73R, A87V, T91V, A129V	This study
pPodA10	<i>Mycobacterium fortuitum podA</i> designed variant cloned into pTEV16 with a TEV cleavable 6X-His tag: I73K, A87V, T91V, A129V, K141T	This study
pPodA11	<i>Mycobacterium fortuitum podA</i> designed variant cloned into pTEV16 with a TEV cleavable 6X-His tag: A53N, I73T, A87V, M99V, A129T	This study
pPodA12	<i>Mycobacterium fortuitum</i> inactive PodA10 cloned into pTEV16 with a TEV cleavable 6X-His tag: A53N, I73T, A87V, M99V, A129T, H121A, E154A, Y156A	This study

<b>Table S3. Primers used in this study</b>	
<b>Primer Name</b>	<b>Primer Sequence 5' → 3'</b>
<b>Overexpression primers</b>	
5' <i>podA</i> pTEV16	NNGCTCTTCNTTCATGGACGGTCGCGGCGGCCGGAGTACAA
3' <i>podA</i> pTEV16	NNGCTCTTCNTAATCATTTCGTCAGTTTCAATTCGTACTTCTC
5' pTEV16 gibson	GCCCTGAAAATACAGGTTTTCACTAGTTG
3' pTEV16 gibson	TAAGAATTCTCGAGCTCCCGGGATC
5' <i>podA</i> gBlock gibson	ATTACGATATCCCAACTAGTGAAAACCTGTATTTTCAGGGC
3' <i>podA</i> gBlock gibson	TGCTCAGCGGCCCGGGATCCCGGGAGCTCGAGAATTCTTA

## SI References

1. Thomsen MCF, Nielsen M (2012) *Seq2Logo*: a method for construction and visualization of amino acid binding motifs and sequence profiles including sequence weighting, pseudo counts and two-sided representation of amino acid enrichment and depletion. *Nucleic Acids Res* 40(Web Server issue):W281-7.
2. VanDrisse CM, Escalante-Semerena JC (2016) New high-cloning-efficiency vectors for complementation studies and recombinant protein overproduction in *Escherichia coli* and *Salmonella enterica*. *Plasmid* 86:1–6.
3. Costa KC, Glasser NR, Conway SJ, Newman DK (2017) Pyocyanin degradation by a tautomerizing demethylase inhibits *Pseudomonas aeruginosa* biofilms. *Science* 355(6321):170–173.